Quantitative Three-Dimensional Structure-Transport Analysis in Chromatographic Beds of Arbitrary Cross-Section

Siarhei Khirevich,[1] Alexandra Höltzel,[1] Dzmitry Hlushkou,[1] Andreas Seidel-Morgenstern,[2] and Ulrich Tallarek[1]

[1]Department of Chemistry, Philipps-Universität Marburg, Hans-Meerwein-Strasse, 35032 Marburg, Germany
E-mail addresses: khirevic@staff.uni-marburg.de, tallarek@staff.uni-marburg.de
[2]Max Planck Institute for Dynamics of Complex Technical Systems, Sandtorstrasse 1, 39106 Magdeburg, Germany

Introduction

The microchannel geometry is mainly determined by the fabrication methods used and inherently non-cylindrical. The cross-sections of LC-microchip separation columns include semicircular, quadratic, rectangular, trapezoidal, and elliptical geometries, often with irregularly-angled corners and curved sides. By employing numerical methods, we investigated an influence of the channel cross-section, interparticle porosity, and fluid velocity on the hydrodynamic dispersion. Numerical simulations were performed on supercomputers and included the following steps: i) packing generation, ii) flow simulation, and iii) hydrodynamic dispersion simulation. We analyzed hydrodynamic dispersion within packings of circular, rectangular, semicircular, and trapezoidal cross-sections. The lateral dimensions and interparticle porosity of the packings were chosen to represent typical values encountered in microchip liquid chromatography systems.

Basic cross-sectional geometries

Figure 1. Porosity (interparticle void fraction) distribution in the near wall region of a cylindrical packing with mean porosity of $\varepsilon_{av} = 0.42$. Comparison with experimental data.

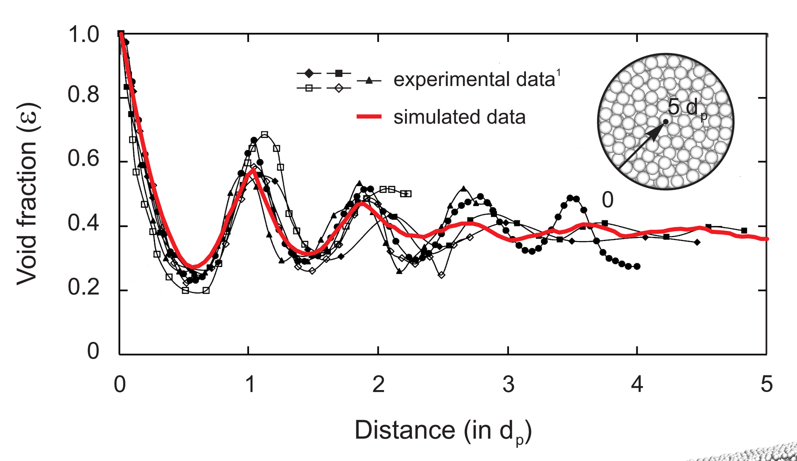

- Confined packings of uniform spherical particles were generated using the Jodrey-Tory approach. Packings were confined by hard walls in the XY-plane and periodic boundary conditions were used along the Z-direction.
- Distribution of porosity near the confining wall agrees well with the experimental data[1] (Figure 1).
- The longitudinal dimension of packings was chosen to avoid the occurrence of recorrelation effects in the simulation[2] (Figure 2).
- The generated packings were discretized with a spatial resolution of 30 nodes per particle diameter (d_p).

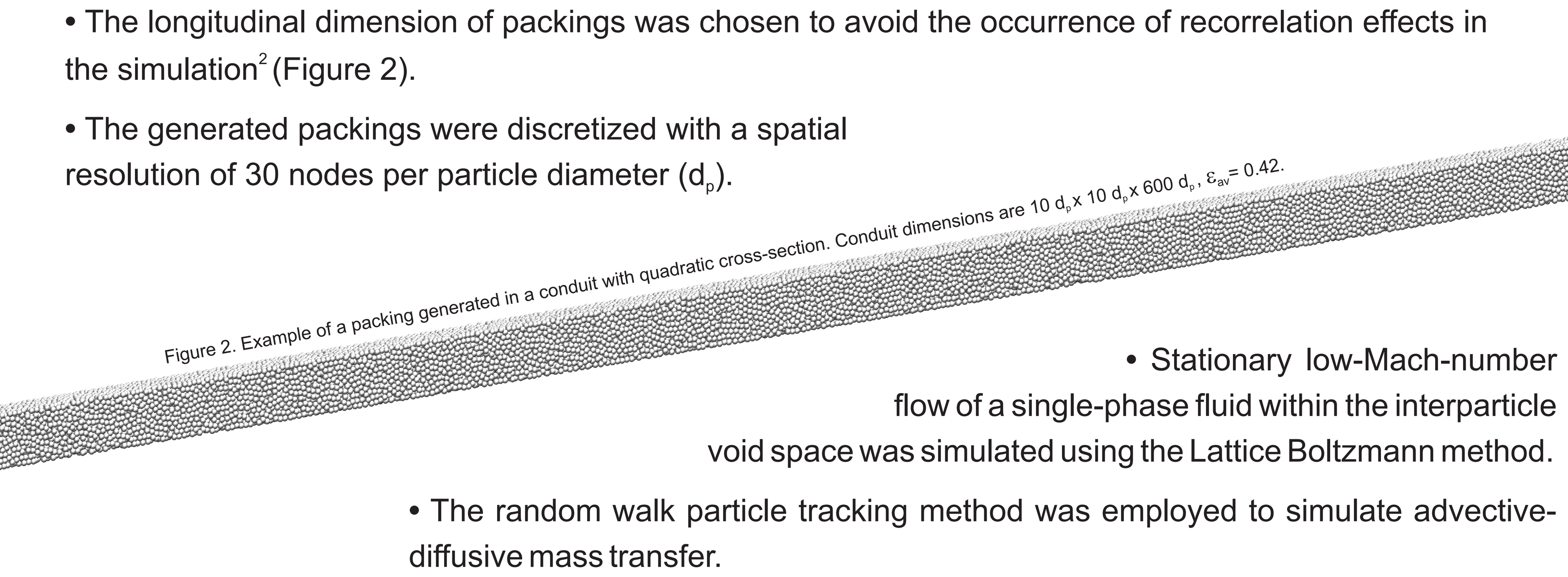

Figure 2. Example of a packing generated in a conduit with quadratic cross-section. Conduit dimensions are $10\,d_p \times 10\,d_p \times 600\,d_p$, $\varepsilon_{av} = 0.42$.

- Stationary low-Mach-number flow of a single-phase fluid within the interparticle void space was simulated using the Lattice Boltzmann method.
- The random walk particle tracking method was employed to simulate advective-diffusive mass transfer.

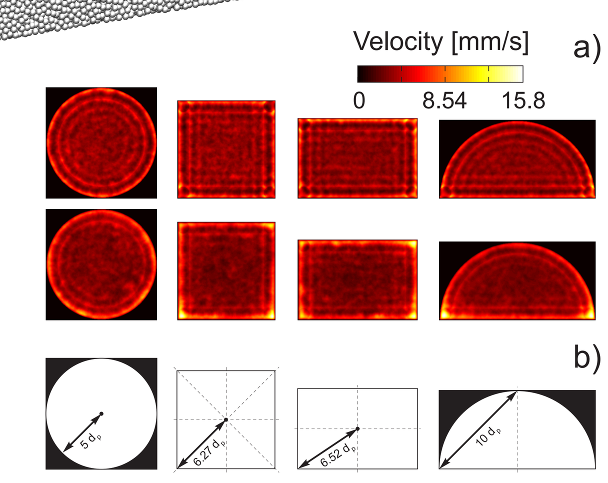

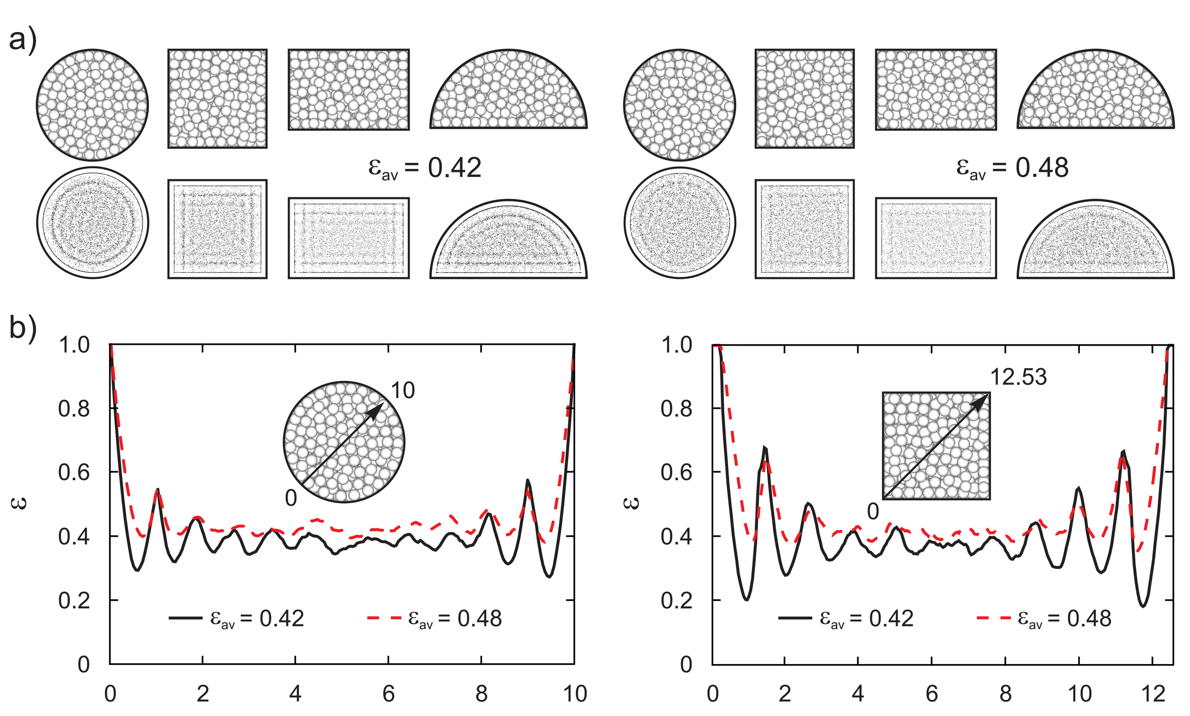

Figure 3. a) Front view of generated packings with basic cross-sectional geometries (top) and projections of particle centers (bottom). The average bed porosity of $\varepsilon_{av} = 0.42$ (left), $\varepsilon_{av} = 0.48$ (right). **b)** Porosity distributions in packings with circular and quadratic cross-section along the indicated arrows at $\varepsilon_{av} = 0.42$ and $\varepsilon_{av} = 0.48$.

- The presence of corners gives rise to the formation of channels of advanced fluid flow velocity[3].
- The reduced symmetry of non-cylindrical packings effects a longer characteristic length of the solute molecules for lateral equilibration between different velocities[3].
- Non-cylindrical packings are much stronger affected by higher bed porosities than cylindrical packings[3].
- At low bed porosities hydrodynamic dispersion of non-cylindrical packings comes close to that of the cylindrical packings[3].

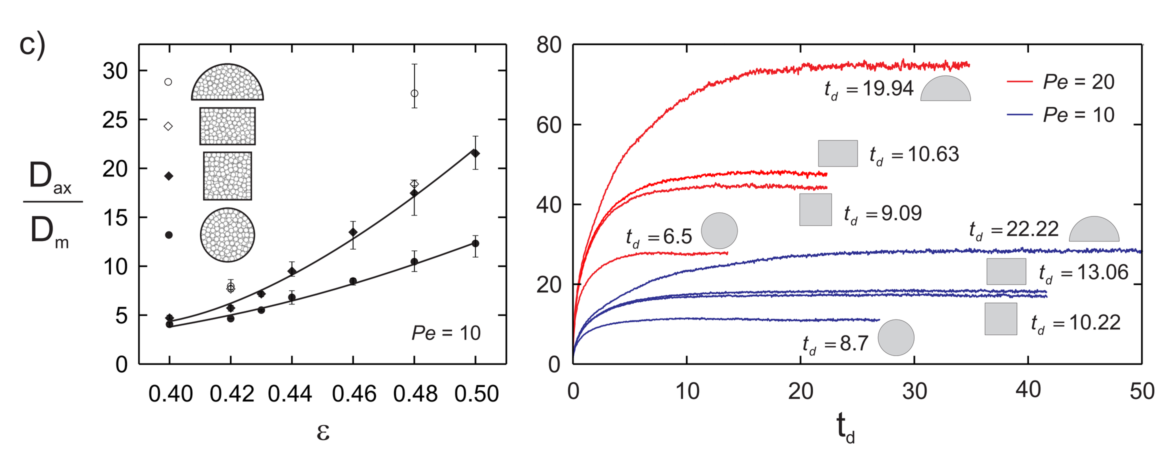

Figure 4. a) Velocity profiles for packings with the basic cross-sectional geometries at two selected bed porosities, $\varepsilon_{av} = 0.42$ and $\varepsilon_{av} = 0.48$. **b)** The schematic illustrates characteristic transverse lengths for each geometry which have to be traversed by the solute molecules in order to realize complete exchange (equilibration) between different velocities. **c)** Left: effective axial dispersion coefficient D_{ax} (normalized by the bulk molecular diffusion coefficient D_m) as a function of the bed porosity simulated for an inert tracer at Pe = 10. For the circular and quadratic packing geometries seven values in the range of $0.40 \le \varepsilon_{av} \le 0.50$ were computed, while for the packed rectangular and semicircular geometries values at two selected bed porosities of $\varepsilon_{av} = 0.42$ and $\varepsilon_{av} = 0.48$ were calculated. Right: Normalized axial dispersion coefficient of an inert tracer as a function of dimensionless diffusive time $t_d = 2D_m t/d_p^2$ for fixed beds with a porosity of $\varepsilon_{av} = 0.48$. For each container geometry two curves are shown, one calculated at Pe = 10 and one at Pe = 20. Each curve represents an average of three independent calculations starting with the generation of packings from three different seeds. The actual values for t_d provided in the figure represent the time for each geometry (and value of Pe) after which asymptotic behavior in D_{ax}/D_m is observed.

Trapezoidal cross-sections

- The limitations of restricted space in the top part of the trapezoidal conduits effect a more ordered, denser packing structure[4].
- With regard to efficiency, trapezoidal packings of larger aspect ratio (width-to-height ratio) are preferable over smaller aspect ratio packings[4].

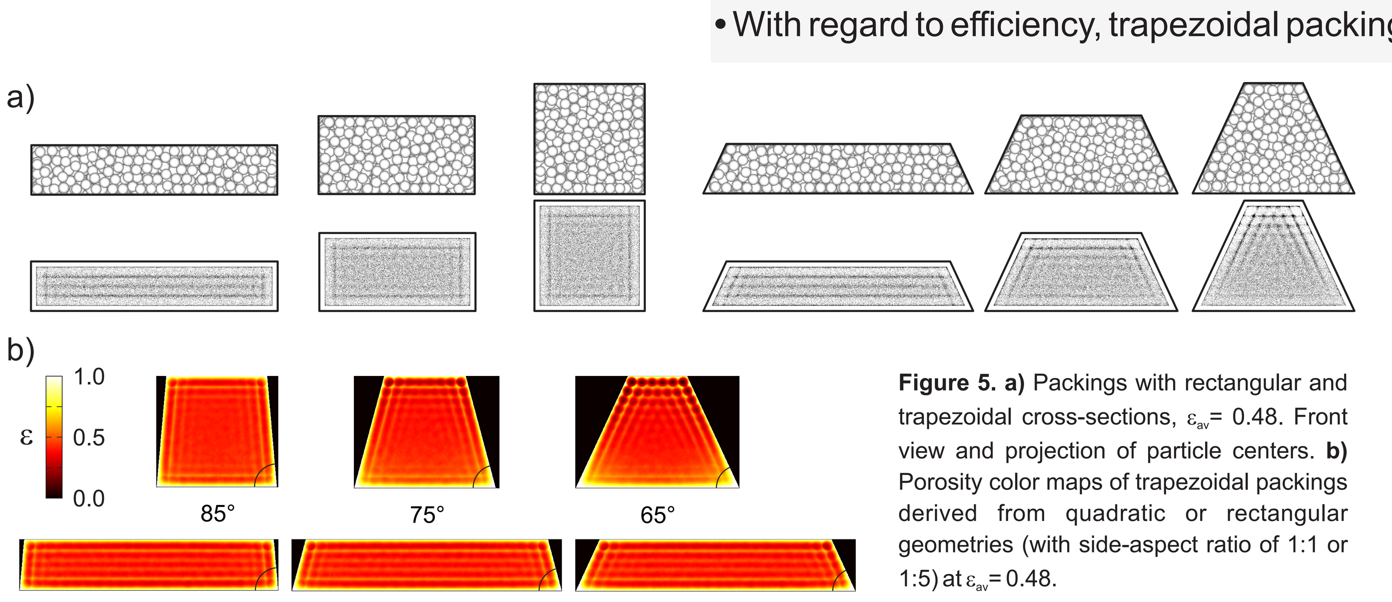

Figure 5. a) Packings with rectangular and trapezoidal cross-sections, $\varepsilon_{av} = 0.48$. Front view and projection of particle centers. **b)** Porosity color maps of trapezoidal packings derived from quadratic or rectangular geometries (with side-aspect ratio of 1:1 or 1:5) at $\varepsilon_{av} = 0.48$.

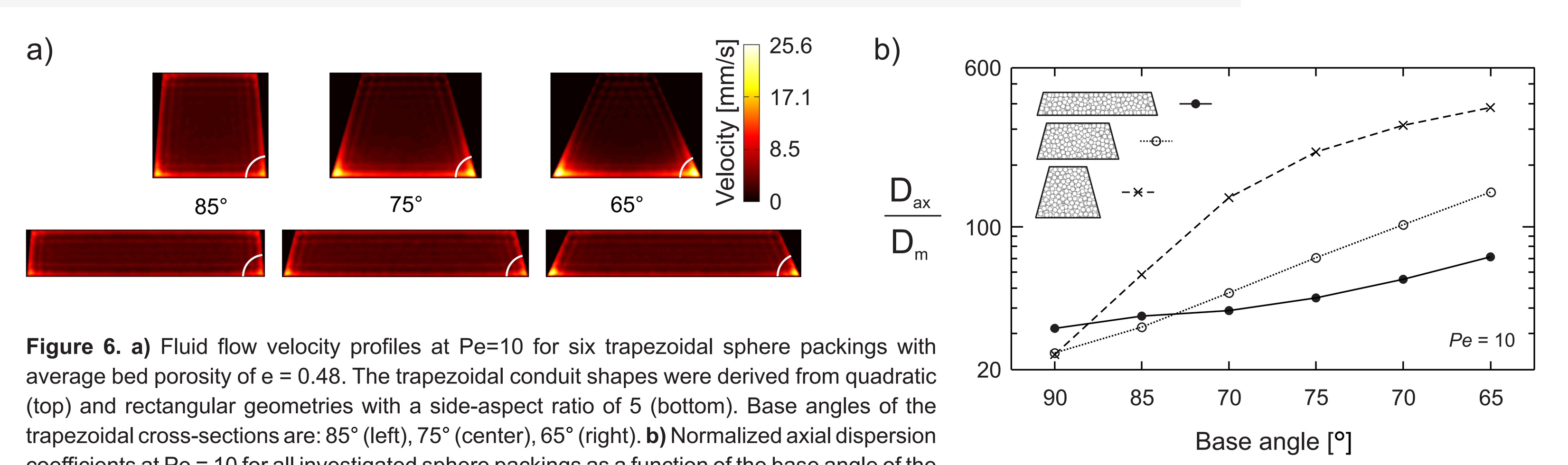

Figure 6. a) Fluid flow velocity profiles at Pe=10 for six trapezoidal sphere packings with average bed porosity of ε = 0.48. The trapezoidal conduit shapes were derived from quadratic (top) and rectangular geometries with a side-aspect ratio of 5 (bottom). Base angles of the trapezoidal cross-sections are: 85° (left), 75° (center), 65° (right). **b)** Normalized axial dispersion coefficients at Pe = 10 for all investigated sphere packings as a function of the base angle of the quadrilateral conduits.

Time and length scales of eddy dispersion[5]

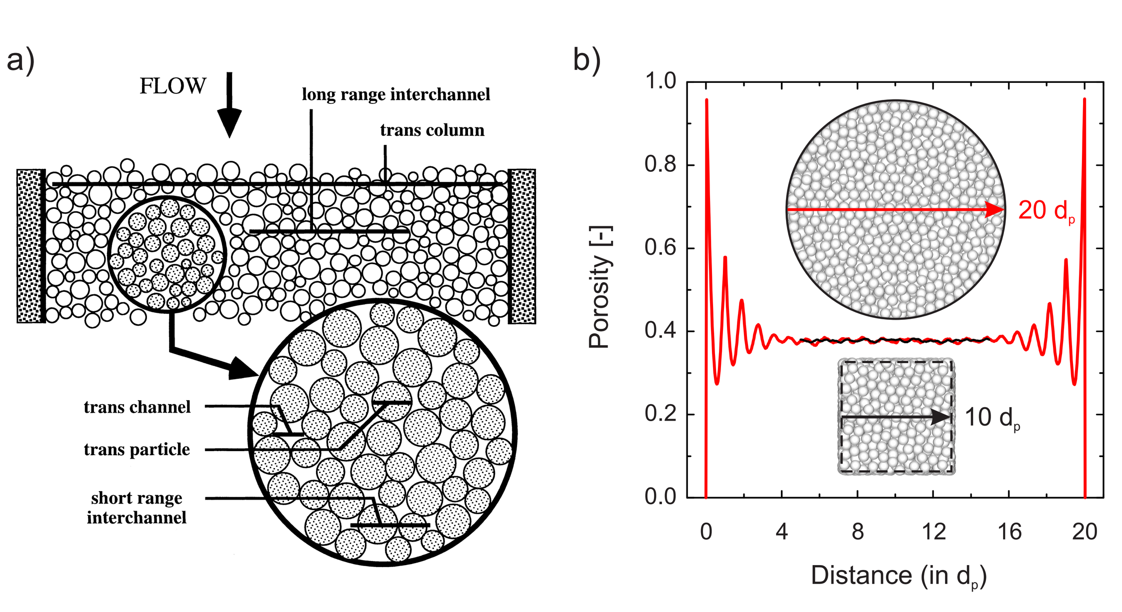

Figure 7. a) Definitions, locations, and scales of the different velocity inhomogeneities contributing to eddy dispersion according to Giddings[6]. Reprinted with permission from Tallarek et al.[7] Copyright 1998 American Chemical Society. **b)** Front view onto the two types of monodisperse sphere packings studied in this work, together with representative lateral porosity distributions (taken along the arrows and averaged over the whole length of the packings). Confined packings have a cylinder-to-particle diameter ratio of $d_c/d_p = 20$, a length of 6553.6 d_p, and a bed porosity of $\varepsilon_{av} = 0.40$. Bulk (unconfined) packings have dimensions of $10\,d_p \times 10\,d_p \times 68.27\,d_p$ with periodic boundary conditions in all directions and a bed porosity of $\varepsilon_{av} = 0.378$.

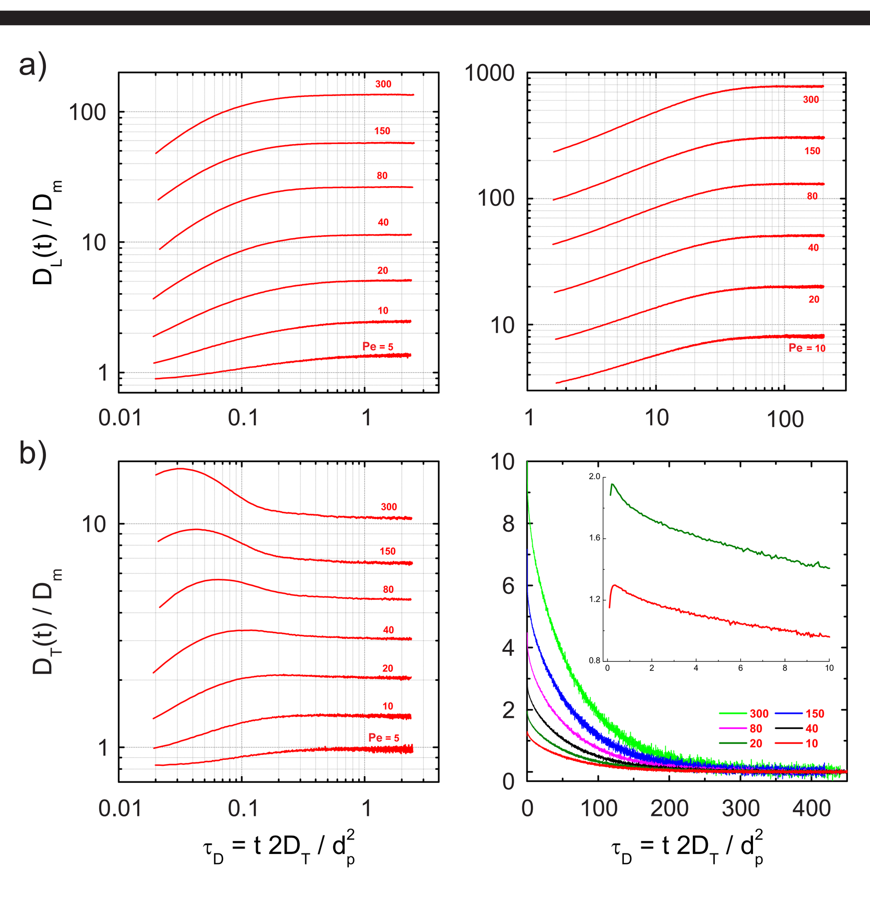

Figure 8. Development of longitudinal (**a**) and transverse (**b**) dispersion coefficients vs. dimensionless transverse dispersive time $\tau_D = 2D_T t/d_p^2$ in bulk (top) and confined cylindrical (bottom) packings ($\varepsilon_{av} = 0.378$). Reduced velocities $Pe = u_{av}d_p/D_m$ ($d_p = 5\,\mu m$, $D_m = 1.5 \times 10^{-9}\,m^2/s$) are given for each curve. **Characteristic average transverse dispersion lengths: $\langle \ell_T \rangle_{bulk} \approx 1.4\,d_p$, $\langle \ell_T \rangle_{confined,\,L} \approx 10\,d_p$, $\langle \ell_T \rangle_{confined,\,T} \approx 20\,d_p$.**

$$h_L = \frac{2\gamma}{Pe} + \overbrace{\frac{2\lambda_1}{1+(2\lambda_1/\omega_1)Pe^{-1}}}^{\text{trans-channel}} + \underbrace{\frac{2\lambda_2}{1+(2\lambda_2/\omega_2)Pe^{-1}}}_{\text{short-range interchannel}} \quad (1)$$

$$h_L = \frac{2\gamma}{Pe} + \overbrace{\frac{2\lambda_1}{1+(2\lambda_1/\omega_1)Pe^{-1}}}^{\text{trans-channel}} + \underbrace{\frac{2\lambda_2}{1+(2\lambda_2/\omega_2)Pe^{-1}}}_{\text{short-range interchannel}} + \underbrace{\frac{2\lambda_3}{1+(2\lambda_3/\omega_3)Pe^{-1}}}_{\text{trans-column}} \quad (2)$$

	γ	λ_1	ω_1	λ_2	ω_2	λ_3	ω_3	R^2
Bulk packings, this work	0.64	0.41	0.0038	0.223	0.15	-	-	0.9998
Confined packings, this work	0.67	0.41	0.0038	0.86	0.436	2.61	0.023	0.9996
Giddings' estimation[6]	-	0.5	0.01	0.5	0.5	0.02 - 10	0.4 - 200	-

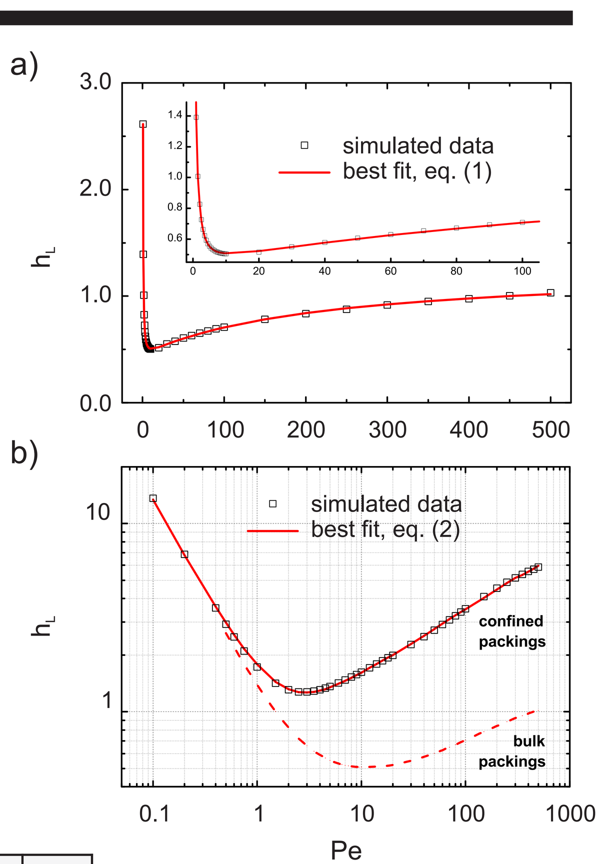

Figure 9. Reduced longitudinal plate height $h_L = H_L/d_p$ vs. reduced velocity $Pe = u_{av}d_p/D_m$ in the range of $0.5 \le Pe \le 500$ for bulk packings (**a**, $\varepsilon_{av} = 0.378$) and $0.1 \le Pe \le 500$ for confined cylindrical packings (**b**, $\varepsilon_{av} = 0.40$). Each data point represents the average from five generated packings.

Acknowledgements

We thank RZG (Rechenzentrum Garching, Germany) and GWDG (Gesellschaft für wissenschaftliche Datenverarbeitung Göttingen, Germany) for providing computational resources and technical support.

References

(1) de Klerk, A. *Voidage variation in packed beds at small column to particle diameter ratio.* AIChE J. **2003**, 49, 2022-2029.
(2) Maier, R. S.; Kroll, D. M.; Bernard, R. S.; Howington, S. E.; Peters, J. F.; Davis, H. T. *Pore-scale simulation of dispersion.* Phys. Fluids **2000**, 12, 2065-2079.
(3) Khirevich, S.; Höltzel, A.; Hlushkou, D.; Tallarek, U. *Impact of conduit geometry and bed porosity on flow and dispersion in noncylindrical sphere packings.* Anal. Chem. **2007**, 79, 9340-9349.
(4) Khirevich, S.; Höltzel, A.; Hlushkou, D.; Seidel-Morgenstern, A.; Tallarek, U. *Structure-transport analysis for particulate packings in trapezoidal microchip separation channels.* Lab Chip **2008**, 8, 1801-1808.
(5) Khirevich, S.; Höltzel, A.; Seidel-Morgenstern, A.; Tallarek, U. *Time and length scales of eddy dispersion in chromatographic beds.* Anal. Chem. **2009**, submitted.
(6) Giddings, J. C. *Dynamics of Chromatography, Part 1: Principles and Theory*; Marcel Dekker: New York, **1965**.
(7) Tallarek, U.; Bayer, E.; Guiochon, G. *Study of dispersion in packed chromatographic columns by pulsed field gradient nuclear magnetic resonance.* J. Am. Chem. Soc. **1998**, 120, 1494-1505.